Journal of Medicinal Chemistry Article

J. Med. Chem. **2009,** *52,* 5217–5227 **5217**
DOI: 10.1021/jm900517t

Identification and Biological Evaluation of a Series of 1*H*-Benzo[*de*]isoquinoline-1,3(2*H*)-diones as Hepatitis C Virus NS5B Polymerase Inhibitors[†,‡]

Jesus M. Ontoria,*[,§] Edwin H. Rydberg,[§] Stefania Di Marco,[§] Licia Tomei,[§] Barbara Attenni,[§] Savina Malancona,[§] José I. Martin Hernando,[§] Nadia Gennari,[§] Uwe Koch,[§] Frank Narjes,[§] Michael Rowley,[§] Vincenzo Summa,[§] Steve S. Carroll,[∥] David B. Olsen,[∥] Raffaele De Francesco,[§] Sergio Altamura,[§] Giovanni Migliaccio,[§] and Andrea Carfì*[,§]

[§]*Istituto Di Ricerche Di Biologia Molecolare, P. Angeletti, S.p.A. (IRBM-MRL Rome), Via Pontina Km 30,600, I-00040 Pomezia, Italy, and* [∥]*Antiviral Research, Merck Research Laboratories, West Point, Pennsylvania 19846*

Received April 23, 2009

The hepatitis C virus (HCV) NS5B RNA-dependent RNA polymerase (RdRp) plays a central role in virus replication. NS5B has no functional equivalent in mammalian cells and, as a consequence, is an attractive target for inhibition. Herein, we present 1*H*-benzo[*de*]isoquinoline-1,3(2*H*)-diones as a new series of selective inhibitors of HCV NS5B polymerase. The HTS hit **1** shows submicromolar potency in two different HCV replicons (1b and 2b) and displays no activity on other polymerases (HIV-RT, Polio-pol, GBV-b-pol). These inhibitors act during the pre-elongation phase by binding to NS5B non-nucleoside binding site Thumb Site II as demonstrated by crystal structure of compound **1** with the ΔC55-1b and ΔC21-2b enzymes and by mutagenesis studies. SAR in this new series reveals inhibitors, such as **20**, with low micromolar activity in the HCV replicon and with good activity/toxicity window in cells.

Introduction

Hepatitis C virus (HCV) is a (+)-stranded RNA virus belonging to the *Flaviviridae* family of enveloped viruses. It is estimated that 180 million people worldwide have been infected by HCV, and two-thirds of them are at risk for developing chronic liver disease, cirrhosis, and hepatocellular carcinoma.[1] Currently the only approved therapy against HCV is pegylated interferon IFN-α (IFN), either as monotherapy or in combination with ribavirin. However, this therapy is poorly tolerated and of limited efficacy.[2]

HCV exhibits a high degree of genetic variability. To date, six genotypes and more than 50 subtypes have been identified, with genotypes 1 and 2 being the most prevalent forms and accounting for more than 13 million cases of disease in the U. S. and Europe combined. HCV genotype is one of the major determinants of the efficacy of treatment. In addtion, it has been found that inherent genotypic differences are responsible for different sensitivities to several small molecule inhibitors.[3]

The HCV RNA genome is 9.6 kb long and codes for a single polyprotein. Polyprotein processing by viral and cellular host factors results in four structural proteins (Core-E1-E2-p7) and six nonstructural (NS) proteins.[4] NS5B is the RNA-dependent RNA polymerase (RdRp) at the core of the HCV replicative complex. The three-dimensional structures of C-terminally truncated forms of NS5B (ΔC21 or ΔC55) from genotypes 1b, 2a and 2b have been determined alone or in complex with a short RNA template or with NTPs.[5] The enzyme shares the same general right-handed fingers, thumb, and palm domain structure of other single-chain polynucleotide polymerase. However, the HCV polymerases has an elongated loop that extends from the fingers domain to make contact with the thumb domain, enclosing the active site cleft and resulting in a spherical appearance for the enzyme.

NS5B is crucial for viral infectivity and is a validated target for the development of therapeutics against HCV. Screening of small molecule libraries has resulted in the discovery of several classes of non-nucleoside inhibitors (NNIs). At least four binding sites have been identified:[6] Thumb Site I[7] and Thumb Site II,[8] located on the surface of the thumb domain at about 30−35 Å from the active site; Palm Site I[5f,9] and Palm Site II[10] are two adjacent and partially overlapping binding sites located in proximity to the enzyme active site cavity. Point mutations conferring resistance to inhibitors binding to each of these sites have been described. Replacement of Pro495 with Ala and Leu, or Leu392 with Ile in binding Thumb Site I have been shown to confer resistance to the Thumb Site I specific indole-acetamide class of inhibitors.[5g,7a,7d] Mutation of Met423 has been shown to confer resistance of the NS5B enzyme to inhibition by compounds binding to Thumb Site II,[11] whereas mutation of Met414 to Thr or Val gave resistance to compounds binding to the internal Palm Site I[11] and Palm Site II,[10a] respectively.

Herein, we report the identification and biochemical characterization of a series of 1*H*-benzo[*de*]isoquinoline-1,3(2*H*)-diones as selective inhibitors of the NS5B polymerase, some of which are effective inhibitors of HCV replication in 1b and 2b replicon assays with no associated toxicity. Several studies on the genotype selectivity, mechanism of inhibition, and binding

[†] PDB codes for the X-ray structures of the ΔC21-2b and ΔC55-1b NS5B polymerase bound to **1** are 3HVO and 2WHO, respectively.

[‡] Dedicated to the memory of Giovanni Migliaccio.

*To whom correspondence should be addressed. For J.M.O.: phone, +39-0691093520; fax, +39-0691093654; e-mail, jesus_ontoria@merck.com. For A.C.: phone, +39-0691093550; fax, +39-0691093654; e-mail, andrea_carfi@merck.com.

Published on Web 07/24/2009

mode are presented. The high resolution crystal structures of one such compound in complex with the NS5B polymerases from genotypes 1b and 2b are also described. Finally, an initial SAR for this class of compounds is discussed in light of the structural data.

Lead Identification

In order to identify compounds that inhibit the HCV NS5B polymerase from more than one genotype, we initiated a high throughput screen (HTS) of our compound collection using two enzyme assays, which utilize the isoforms ΔC21-1b (BK strain) for genotype 1 and ΔC21-2b (2b.2 strain) for genotype 2.[7a] This HTS campaign led to the identification of **1** as a submicromolar inhibitor of both genotypes 1 and 2 NS5B polymerase. The compound was also an effective inhibitor of HCV replication in the Huh7 clone HBI10A expressing the 1b-Con1 replicon (HEPREP 1b)[12] and in the H2B2 clone expressing a chimeric replicon carrying the NS5B-2b enzyme in the context of the 1b (BK) replicon (HEPREP 2b) with a 10-fold activity/toxicity window in cells (Figure 1). Compound **1** represented an HCV NS5B polymerase inhibitor with a novel chemotype and prompted us to characterize its biological profile and mechanism of inhibition.

Chemistry

Activity validation for our hit compound **1** was accomplished via resynthesis and retesting. The synthesis of **1** was based on the condensation of commercially available 6-bromo-1*H*,3*H*-benzo[*de*]isochromene-1,3-dione **2a** with 3-bromoaniline. When this reaction was performed by heating in NMP at 145 °C for 24 h to obtain the completion of the reaction, the intermediate **3a** was obtained with moderate yields.[13] Use of microwave irradiation increased the yield and shortened the reaction time (200 °C, 30 min). Introduction of the 2-hydroxyethylamine fragment was achieved by Ullman reaction of intermediate **3a** with ethanolamine under microwave irradiation, affording **1**.[14] Compounds **4**−**9** and **12**−**20** were prepared by using the synthetic route described in Scheme 1.

The 2,3-dihydro-1*H*-benzo[*de*]isoquinolin-1-one **10** was prepared by treatment of compound **1** with $NaBH_4$ that led to the selective reduction of the carbonyl group in position 1 of the tricyclic scaffold.[15] Reaction of **1** with BH_3 in THF at reflux gave **11** by reduction of both carbonyl groups (Scheme 2).

HCV and Genotype Selectivity

When tested on purified NS5B polymerases from all the major HCV genotypes, compound **1** appeared active in the submicromolar range on all the enzymes. Differences were observed among the genotypes with a major shift (38-fold) on genotypes 2a and 3a with respect to genotype 1b and only a 10-fold difference for genotype 2b (Table 1).

Compound **1** was also shown to be strictly selective for the HCV polymerase, since it was unable to inhibit at concentrations up to 50 μM the in vitro activity of closely related polymerases such as HIV-RT, GBV[a]-b-NS5B, BVDV RdRp, and Polio-pol (Table 1). Altogether, these results indicate that compound **1** is an HCV selective inhibitor able to affect viral replication of 1a, 1b, and 2b genotypes.

[a] Abbreviations: GBV, GB virus; BVDV, bovine diarrhea virus.

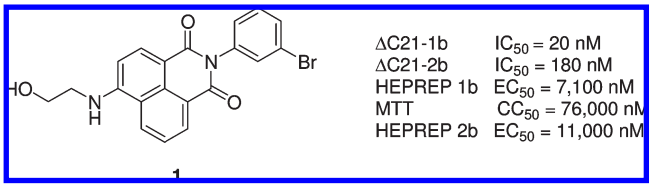

1

Figure 1. Structure of compound **1** and inhibition potency on the purified NS5B ΔC21-1b and ΔC21-2b enzymes and on the replicon HEPREP 1b and 2b assays.

Physicochemical and Pharmacokinetic Profile

The lipophilic structure of **1** was reflected in the slightly high log *D* (log *D* = 3.45) and low solubility (0.44 μg/mL) of the compound. However, when **1** was dosed in rat at 3 mg/kg orally (po), an excellent oral bioavailability (F = 83%) together with high exposure (AUC = 9.7 μM·h) was observed. Peak plasma concentrations, C_{max} = 4.0 μM, occurred after 0.7 h from administration. Moreover, despite a short elimination half-life ($t_{1/2}$ = 0.7 h), a low clearance (Cl = 12 (mL/min)/kg) and a good volume of distribution (V_{dss} = 1.1 L/kg) were observed after iv administration. Globally these results showed that compound **1** had a good overall profile and represented a valid lead for a drug discovery optimization program.

Mechanism of Inhibition of NS5B Polymerase

The study of the mechanism of inhibition indicated that compound **1** acts during the pre-elongation phase, similar to that previously observed for several other NNIs of the HCV polymerase.[7a,7e,16] In fact, complete inhibition of the ΔC21-1b enzymatic activity could not be achieved if the inhibitor was added to a preformed enzyme−RNA complex and a significant fraction of the polymerase activity could not be inhibited even at very high compound concentrations (Figure 2A). This result suggests that the fraction of NS5B engaged with the RNA in a pre-elongation complex is protected from the action of the inhibitor. This hypothesis is further supported by the observation that increasing the preincubation time of the enzyme with the RNA template previous to the addition of compound **1**, at more than 30-fold of its IC_{50}, resulted in an increased residual polymerase enzymatic activity (Figure 2B). As previously observed,[16] the enzyme activity in the absence of inhibitor also increased as preincubation time with the RNA template increased, likely reflecting the formation of a productive pre-elongation complex (data not shown). Presumably, the residual inhibition after longer preincubation time results from those polymerase molecules that dissociated from the template during the elongation reaction and thus become susceptible to inhibition. Indeed, in reactions performed in the presence of heparin as a trapping agent for free enzyme, preincubation with template completely protected the NS5B RdRp from inhibition (Figure 2C). Equivalent results were obtained for the HCV NS5B enzyme from genotype 2b (data not shown).

Elucidation of Binding Site of Compound 1

In order to identify the binding site of compound **1**, its efficiency was evaluated initially on ΔC21-1b RdRp carrying mutations able to confer resistance to inhibition by molecules known to interact with different sites on the enzyme. As reported in Table 2, the Thumb Site II mutants M423K and R501E, but not the Palm Sites I and II mutant M414T, appeared highly resistant to compound **1** as well as to

Scheme 1. Synthesis of Compounds **1**, **4**−**9**, and **12**−**20**[a]

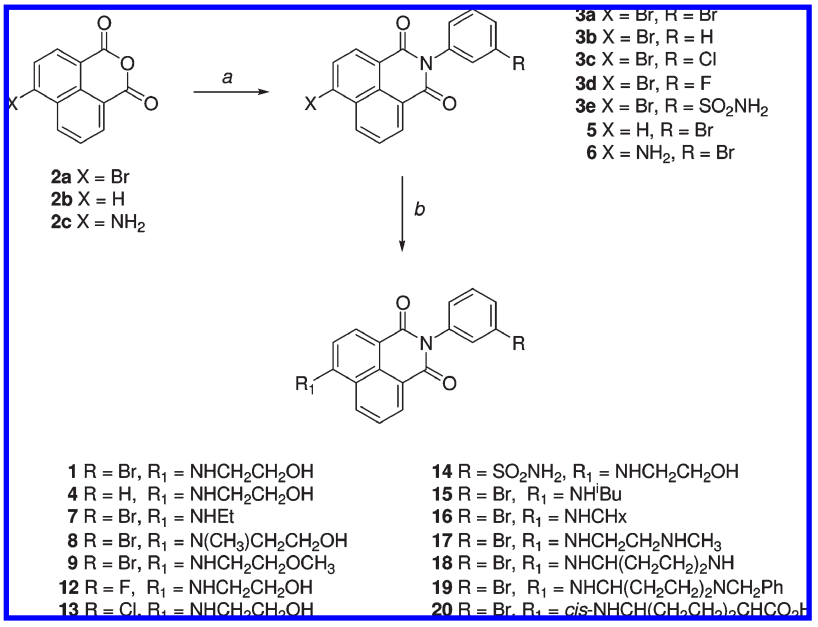

[a] Reagents and conditions: (a) $ArNH_2$, NMP, microwave, 200 °C, 30 min; (b) $R'NH_2$, NMP, microwave, 200 °C.

Scheme 2. Synthesis of Compounds **10** and **11**[a]

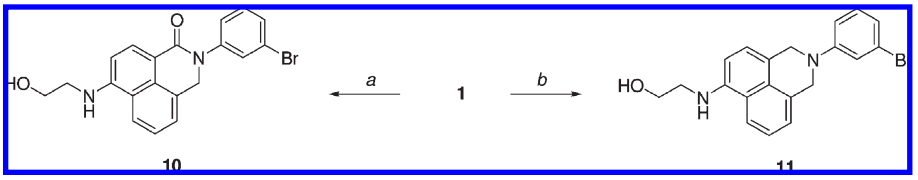

[a] Reagents and conditions: (a) $NaBH_4$, $EtOH/H_2O$, room temp; (b) BH_3, THF, reflux.

Table 1. Activity of Resynthesized Compound **1** on the Purified NS5B ΔC21 Enzymes of Different HCV Genotypes (First Three Columns), on Huh7 Clones Carrying Replicons from the Indicated Genotypes (Middle Two Columns), and on HCV-Unrelated Polymerases (Last Two Columns)

NS5B ΔC21[a]			replicon cell, ELISA[a]		selectivity	
genotype	IC_{50} (μM)	shift vs 1b	genotype	EC_{50} (μM)	polymerase	IC_{50} (μM)
1a RB5	0.064	3.2	H77-1a	4.7	3Dpol	> 50
1b (BK)	0.020	1	1b-BK	4.6	Klenow	> 50
2a.4	0.77	39	1b-Con1	6.4	HIV-RT	> 50
2b.2	0.19	9.5	2b.2	11.1	GBV-b NS5B	> 50
3a.7	0.76	38			BVDV RdRp	> 50
4a	0.54	27				
6a	0.49	25				

[a] Values are the mean of two or more experiments. SD values are ±30% of the mean value.

compound **21**, a NS5B inhibitor with a thiophene scaffold that has been shown to bind to Thumb Site II.[5f,8a] Of note, whereas compound **21** showed a 4-fold loss of enzymatic inhibition to the Thumb Site I P495A mutation, compound **1** potency was not affected. Finally, titration experiments showed that compound **21** was able to compete for inhibition by compound **1** (not shown), confirming that the thiophene inhibitor **21** and compound **1** share the same binding site, Thumb Site II. Importantly, compound **1** represents the first Thumb Site II NS5B inhibitor with a non-acid chemotype.

Crystal Structures of Genotypes 1b and 2b NS5B Bound to Compound 1

The structures of the genotypes ΔC55-1b and ΔC21-2b polymerase in complex with compound **1** were obtained by soaking the crystals with the inhibitor for several hours prior to data collection. The structures were determined by the molecular replacement method and refined up to 2.0 Å resolution (Supporting Information Table S1). Both structures indicated that compound **1** binds at the polymerase Thumb Site II in proximity of Met423 (Figure 3A,B).

In both structures, the inhibitor binds the enzyme in a similar fashion and establishes very similar interactions (Figure 3B). Indeed, only four conservative amino acid differences between genotypes 1b and 2b HCV polymerase are located at this site: Ile419Leu, Thr476Ser, Leu482Ile, and Lys501Arg (2b/1b; Figure 3B). Furthermore, a superposition of these inhibited structures with those of the respective noninhibited enzymes reveals no major changes induced by compound **1** binding except for the displacement of few

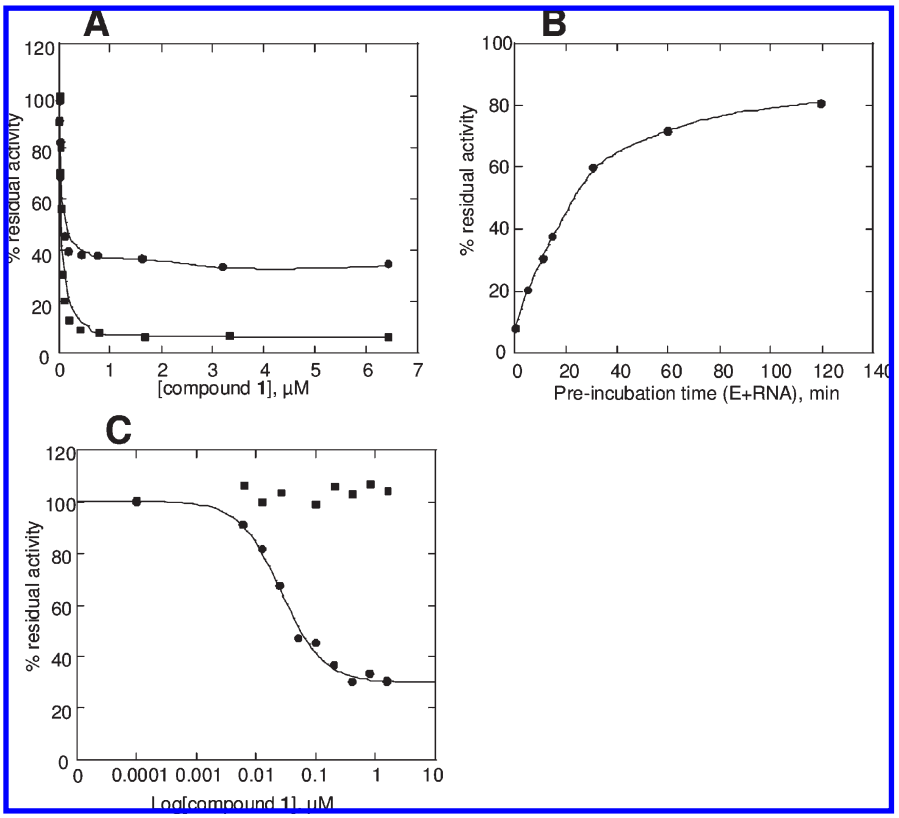

Figure 2. (A) Order of addition. Increasing amounts of compound **1** (3 nM to 6.4 μM) were added to ΔC21-1b polymerase (20 nM) and polyA/oligoU_{18} RNA that were (●) or were not (■) preincubated 15 min at room temperature. (B) Preincubation time course. The NS5B ΔC21-1b and the polyA/oligoU_{18} RNA were preincubated from 0 to 120 min before the addition of 1 μM compound **1**. (C) Inhibition curves by compound **1** in single cycle conditions. The NS5B ΔC21-1b and the polyA/oligoU_{18} RNA were preincubated 5 min before the addition of compound **1** from 0.1 nM to 1 μM. Elongation was started by the addition of ^{3}H-UTP together with (■) or without (●) heparin (50 ng/μL).

Table 2. Structure and Activity of Compounds **1** and **21** on the Wild-Type (wt) NS5B ΔC21-1b Enzyme and Mutants Resistant to Inhibitors Binding at Thumb Site I (P495A), Thumb Site II (R501E and M423K) and Either Palm Site I or II (M414T)[a]

		ΔC21-1b enzyme, IC_{50} (μM)				
			Thumb Site I	Thumb Site II		Palm Site I and II
Compd	Structure	wt	P495A	R501E	M423K	M414T
1	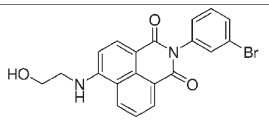	0.02	0.02	0.5	> 1	0.078
21	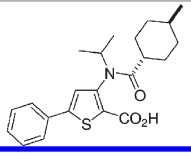	0.009	0.04	0.1	> 0.5	0.016

[a] Values are the mean of two or more experiments. SD values are ±30% of the mean value.

ordered water molecules (Figure 3A) and the repositioning of the side chains of Arg498 and Arg501 in the 1b enzyme (not shown).

The inhibitor binds at the center of a long cleft that is approximately 30 Å long, 10 Å wide, and 10 Å deep. The side chains of Arg422, Trp528, Met423, Ile419 (Leu in 1b), Tyr477, and Leu497 contribute to the formation of the floor of the inhibitor binding cleft, whereas the rims are formed in the upper part by the side chains of Lys501 (Arg in 1b) and Arg498 and at the bottom by the side chains of Leu482 and Ala486 and the backbone atoms of residues 474−477 (Figure 3B). The inhibitor establishes a large number of van der Waals and hydrophobic interactions with the protein mainly via the tricyclic moiety, the phenyl group, and the bromine substituent. In particular, the bromine atom and the phenyl ring fill completely a small deep pocket formed by the side chains of Trp528, Ile419, Tyr477, Met423, and Arg422 (Figure 3C). The interaction between compound **1** and the enzyme is also characterized by the presence of several H-bonds, most of which are water-mediated (Figure 3A). In the 2b structure, one carbonyl oxygen of the tricyclic moiety forms a water-mediated H-bond with the side chain of Lys501,

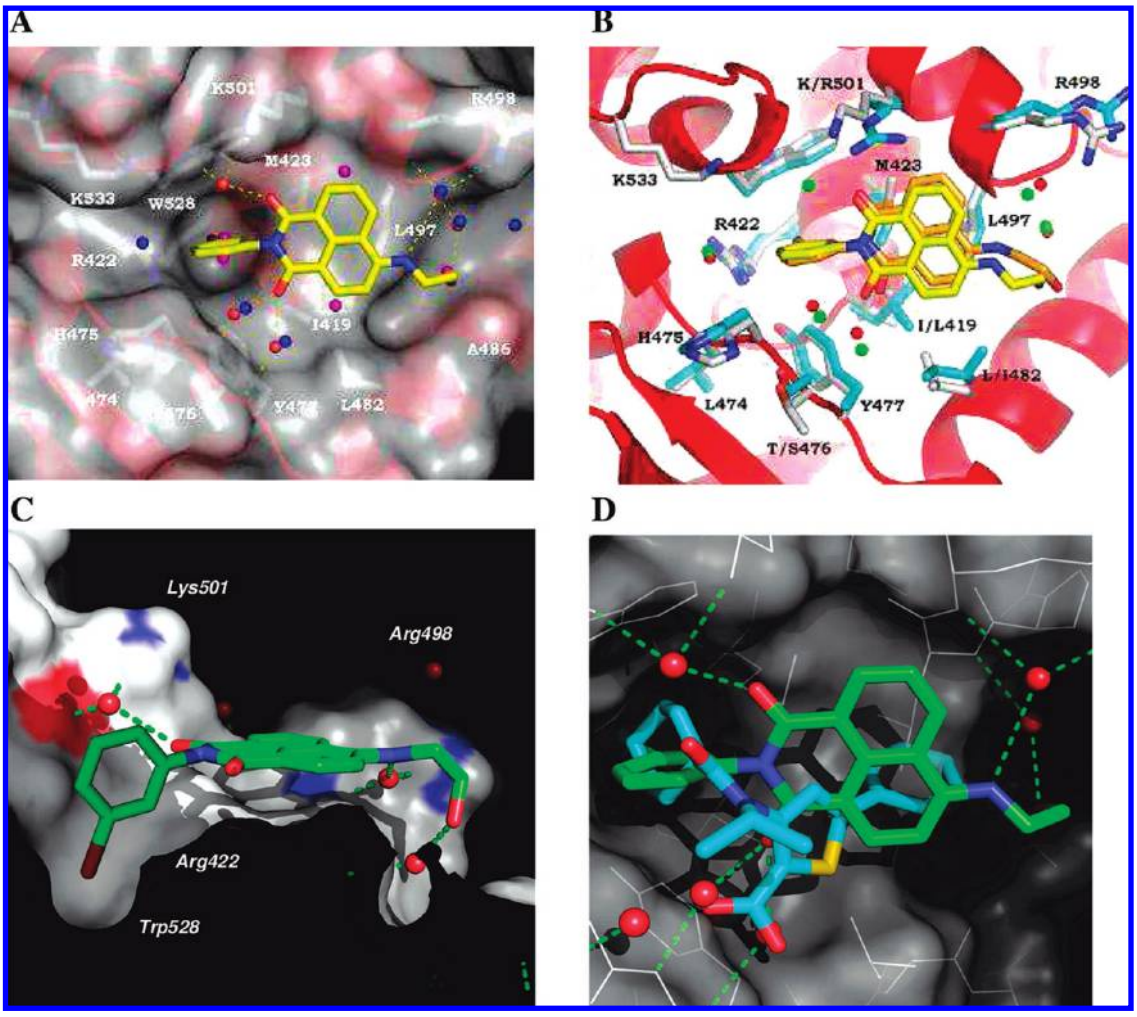

Figure 3. Structure of NS5B−**1** complex. (A) The inhibitor binding cleft in the ΔC21-2b polymerase. The inhibitor and residues forming the binding site are in stick representation. Carbon, oxygen, and nitrogen for the inhibitor are yellow, red, and blue, respectively. Carbon, oxygen, and nitrogen for the protein are gray, red, and blue, respectively. Water molecules in the inhibited ΔC21-2b and ΔC55-1b polymerase structures are shown as red and blue spheres, respectively. Water molecules in the noninhibited ΔC21-2b polymerase are shown as magenta spheres. H-Bonds are represented by dashed, yellow lines. (B) Comparison of inhibited ΔC55-1b and ΔC21-2b polymerase structures. Water molecules in the 1b and 2b polymerase structures are shown as red and green spheres, respectively. (C) Picture of compound **1** docked in the Thumb Site II binding pocket of the ΔC21-2b polymerase. The interactions of compound **1** with the lipophilic pocket on the inhibitor binding cleft and the water-mediated H-bonds formed with Lys501 and Arg498 are shown. (D) Compound **21** docked on the structure of compound **1**/ΔC21-2b complex. Water molecules are shown as red spheres.

whereas in the 1b structure, this water molecule is absent and the same oxygen establishes a direct H-bond with the bulkier side chain of Arg501 (Figure 3B). The second carbonyl oxygen of the inhibitor forms in both structures water-mediated H-bonds with the main chain nitrogens of Tyr477 and Thr476 (Ser476 in 1b). Finally, the −NH and −OH groups of the ethanolamine extension form H-bonds with the side chain guanidinium group and the main chain carbonyl oxygen of Arg498 through three bridging water molecules (Figure 3B, C). We also calculated the intermolecular binding energy of our compound **1** with the NS5B enzyme using the MMFF forcefield,[17] as implemented in Macromodel 7.0,[18] obtaining a value of $\Delta E_{inter} = -271$ kJ/mol. Calculation of the intermolecular binding energy for analogue **4**, which is devoid of the bromine atom, gave a value of $\Delta E_{inter} = -196$ kJ/mol. Moreover, the value obtained for the molecule without the bromophenyl group is $\Delta E_{inter} = -31$ kJ/mol. These value's differences reflect the importance of the lipophilic interactions of the bromine atom and the phenyl ring with the side chains of the amino acids that form the small deep pocket. To compare the interactions established by compounds **1** and **21** with the NS5B polymerase, we docked the latter compound into the Thumb Site II pocket of the ΔC21-2b enzyme. The docking of **21** was performed using the crystal structure of the ΔC21-2a polymerase bound to a structurally closely related compound (PDB ID code 1YVX) as template. The superposition reveals that the methylcyclohexyl group of **21** binds to the same small lipophilic pocket as the bromophenyl group of compound **1** (Figure 3D). Moreover, the two oxygen atoms of the carboxylate of **21** occupy the same position occupied in structure of the ΔC21-2b/**1** complex by two water molecules that form hydrogen bonds with one of the carbonyl oxygens of the inhibitor and with the main chain nitrogens of Tyr477 and Thr476.

SAR Studies

In parallel with the structural and functional characterization of the hit compound **1**, we initiated SAR studies to identify the pharmacophoric elements of this class of compounds that are essential for NS5B polymerase binding and

Table 3. Enzymatic Activity of Compounds **1** and **4**−**11**

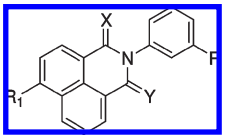

Compd	X	Y	R	R_1	ΔC21-1b BK IC_{50} (nM)[a]	ΔC21-2b.2 IC_{50} (nM)[a]
1	O	O	Br		20	180
4	O	O	H		1,700	> 50,000
5	O	O	Br	H	> 50,000	> 50,000
6	O	O	Br	NH_2	190	300
7	O	O	Br		29	185
8	O	O	Br		500	1,800
9	O	O	Br		24	124
10	O	H_2	Br		850	3,500
11	H_2	H_2	Br		> 50,000	> 50,000

[a] Values are the mean of two or more experiments. SD values are ±30% of the mean value.

inhibition. With this purpose, we initially prepared a series of analogues of **1** that were devoid of one of its structural features (Table 3).

In agreement with the X-ray structures, the debrominated analogue **4** displayed a loss of 2 orders of magnitude in potency, highlighting the relevance of the bromine atom for the lipophilic interaction of **1** with the binding pocket formed by Trp528, Ile419, Tyr477, Met423, and Arg422. Similarly, removal of the ethanolamine fragment as in **5**, which in the structure of the complex establishes both apolar and polar and H-bond interactions with residues forming the cleft, led to a complete loss of inhibition. An important fraction of this inhibitory activity was recovered by introduction of an amino group in position 6 of the tricyclic system, as demonstrated by compound **6**, in line with the H-bond observed in the crystal structure between the NH group of **1** and Arg498. A further improvement in inhibition potency, particularly against the genotype 1b, was observed by the introduction of an ethyl chain as in compound **7**. The N-methylated analogue **8** showed a 25-fold loss of enzymatic activity, further confirming the importance of the H-bond with Arg498. Methylation of the hydroxyl group, as in **9**, did not affect significantly potency, and it led to a moderate decrease in genotype selectivity. The importance of the H-bonds between the compound carbonyl oxygens and the side chains of Lys501 (Arg501 in 1b) and the main chain nitrogens of Tyr477 and Thr476 (Ser476 in 1b) was demonstrated by compounds **10** and **11**, where elimination of one or two of the carbonyl groups led to a very significant or complete loss of inhibition. Overall, the SAR demonstrated that the presence of the bromine atom, the carbonyl groups, and the alkylamine fragment is determinant for the interaction between the lead compound **1** and the HCV NS5B polymerase and is in agreement with the crystal structure of compound **1** bound to ΔC55-1b and ΔC21-2b enzymes. With the aim of increasing the inhibitory activity against both genotypes, we performed additional SAR studies by exploring alternative substituents in the phenyl ring and in the amino group of the tricyclic core (Table 4).

As expected, the replacement of the bromine atom by chlorine as in **12** did not affect inhibition, indicating that the chlorine atom retains most of the lipophilic interactions with the small deep pocket on the NS5B Thumb Site II surface (Figure 3C). In contrast, introduction of smaller halogen such as fluorine (**13**) resulted in a 10-fold loss of potency, and the introduction of polar groups such as the sulfonamide (**14**) led to a relevant decrease of potency on both genotypes of NS5B polymerase (IC_{50} = 1,600 nM, ΔC21-1b). The latter result is not surprising and is consistent with the hydrophobic nature of the bromine binding pocket. As demonstrated by analogue **9** (Table 3), where the aliphatic ethylamine maintains a good level of intrinsic potency, branched alkylamines such as isobutylamine or cyclohexylamine, as in compounds **15** and **16**, showed a little loss of potency against genotype 1 enzyme while maintaining a similar potency against genotype 2, thus resulting in molecules that inhibit both genotypes similarly. Introduction of a basic center in the amino substituent, as in **17**, led to a 7-fold loss of inhibitory activity against genotype 1, which was partially recovered by inclusion of the amino group in a piperidine ring (**18**), probably due to additional lipophilic interaction with the protein established by the six-membered

Table 4. Enzymatic and Cell-Based Activity of Compounds **1** and **12**−**21**

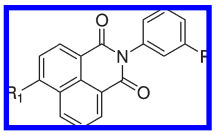

Compd	R	R_1	ΔC21-1b BK IC_{50} (nM)[a]	ΔC21-2b.2 IC_{50} (nM)[a]	HEPREP 1b EC_{50} (nM)[a]	MTT CC_{50} (nM)[a]
1	Br		20	180	7,100	76,000
12	Cl		19	200	3,800	57,000
13	F		200	> 50,000	> 50,000	> 50,000
14	SO_2NH_2		1,600	> 50,000	> 50,000	> 50,000
15	Br		130	90	11,000	> 50,000
16	Br		66	120	> 50,000	> 50,000
17	Br		130	400	2,000	1,500
18	Br		30	120	1,900	3,500
19	Br	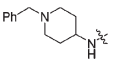	< 14	43	2,200	5,200
20	Br		42	110	3,800	> 50,000
21[b]			9	> 10,000	1,400	> 50,000

[a] Values are the mean of two or more experiments. SD values are ±30% of the mean value. [b] Structure of compound **21** is shown in Table 2.

ring. Introduction in the piperidine ring of a bulky group such as benzyl (**19**) led to a very potent inhibitor with low nanomolar potency against genotype 1 enzyme. This finding is consistent with the X-ray structures that suggest that additional lipophilic contacts can be established with residues forming the elongated inhibitor binding cleft by further extending the inhibitor on the position 6 of the tricyclic system. Unfortunately, the compounds bearing a basic center in their structure were cytotoxic in cells. Compounds that possess a 1*H*,3*H*-benzo[*de*]isochromene-1,3-dione core and bear a basic amine in their structures are reported to be good DNA intercalators,[19] and this could be the reason for the toxicity in the replicon cells. This finding prompted us to look for alternative groups that could abolish binding to DNA. One approach was the introduction of a carboxylate group to reduce the intercalation properties of these compounds by electrostatic repulsion with the phosphate groups of the DNA chain. Introduction of a carboxylic group in the amino substituent, as in **20**, resulted in a compound that, similar to analogue **16**, maintained nanomolar activity against both genotypes and displayed low micromolar inhibition in cells and showed at least a 13-fold window respect to cytotoxicity. When compound **21** was tested on the ΔC21-2b enzyme, no inhibiton was observed up to 10 μM, showing a more than 3 orders of magnitude difference in inhibitory activity compared to genotype 1 (Table 4). Interestingly, although compounds **1** and **21** establish some common interactions with the NS5B polymerase, they showed very different genotype selectivity profile on genotypes 1b and 2b.

Conclusion

A HTS campaign led to the identification of compound **1**, an HCV inhibitor with a novel chemotype, which inhibits NS5B polymerases from all the major HCV genotypes at submicromolar concentrations. Compound **1** is an effective inhibitor of HCV replication in 1b and 2b replicons with a 10-fold activity/toxicity window in cells and excellent selectivity over a panel of closely related polymerases. Experiments aimed at clarifying the mechanism of inhibition showed that **1** acts by binding to NS5B polymerase during the pre-elongation phase. X-ray structures of **1** with NS5B ΔC55-1b and ΔC21-2b show that this compound binds to the non-nucleoside binding site Thumb Site II establishing a large number of van der Waals and hydrophobic interactions with the protein via the tricyclic core and the phenyl group with the bromine substituent filling a small deep pocket. In addition, the polymerase establishes a number of direct and water-mediated H-bonds, where the number varies depending on genotype, with the carbonyl oxygens of the inhibitor. The relevance of these interactions was confirmed by the preparation of analogues that lacked some of these key structural motifs leading to analogues that showed a relevant loss of enzymatic activity. Further SAR in the aromatic ring and in the amino group led to compounds with slightly improved activity in the replicon assay and good activity/toxicity window in cells.

Experimental Section

Chemistry. Solvents and reagents were obtained from commercial suppliers and were used without further purification.

Organics extracts were dried over anhydrous sodium sulfate (Merck). Flash chromatography purifications were performed on Merck silica gel (200−400 mesh) as the stationary phase or were conducted using prepacked cartridges on a Biotage system, eluting with petroleum ether/ethyl acetate or toluene/acetone mixtures. Microwave irradiation was performed in a Personal Chemistry (now Biotage) optimizer, model Emrys. Purity of the compounds was determined by analytical RP-HPLC, data were obtained by two methods on an Acquity Waters UPLC using a flow rate of 0.5 mL/min, an Acquity UPLC BEH C_{18}, 1.7 μm, 2.1 mm × 50 mm column as the stationary phase, and a mobile phase comprising MeCN + 0.1% HCO_2H (solvent A) and H_2O + 0.1% HCO_2H (solvent B). Method 1 parameters are 30% solvent A (0.0 min) to 100% solvent A (2.6 min) and then 100% solvent A (0.3 min). Method 2 parameters are 0% solvent A (0.0 min) to 100% solvent A (2.6 min) and then 100% solvent A (0.3 min). All the compounds described in this article showed purities higher than 95% in both analytical methods. HPLC−MS was performed on a Waters Alliance 2795 apparatus equipped with a diode array and a ZQ mass spectrometer using an X-Terra C_{18} column (5 μm, 4.6 mm × 50 mm). Mobile phase comprised a linear gradient of binary mixtures of H_2O containing 0.1% formic acid (solvent A) and MeCN containing 0.1% formic acid (solvent B). Nuclear magnetic resonance spectra (^{1}H NMR recorded at 500, 400, or 300 MHz, ^{13}C NMR recorded at 100 or 75 MHz) were obtained on Bruker AMX spectrometers and are referenced in ppm relative to TMS. Unless indicated, spectra were acquired at 300 K. High resolving power accurate mass measurement electrospray (ES) mass spectral data were acquired by use of a Bruker Daltonics apex-Qe Fourier transform ion cyclotron resonance mass spetrometer (FT-ICR MS). External calibration was accomplished with oligomers of polypropylene.

6-Bromo-2-(3-bromophenyl)-1*H*-benzo[*de*]isoquinoline-1,3(2*H*)-dione (3a). 3-Bromoaniline (1.2 mL, 10.82 mmol) was added to a solution of **2a** (2.0 g, 7.21 mmol) in NMP (10 mL). The reaction mixture was stirred at 200 °C under microwave irradiation for 30 min. The resulting precipitate was filtered, washed subsequently with EtOH and Et_2O, and dried to give **3a** (2.0 g, 64%) as a pale-brown solid. ^{1}H NMR (300 MHz, DMSO-d_6) δ 8.64−8.58 (m, 2H), 8.36 (d, J = 7.7 Hz, 1H), 8.28 (d, J = 8.0 Hz, 1H), 8.07−8.02 (m, 1H), 7.70−7.67 (m, 2H), 7.53−7.43 (m, 2H); HRMS (ESI) m/z calcd for $C_{18}H_{10}Br_2NO_2$ 429.9073, found 429.9079.

2-(3-Bromophenyl)-6-[(2-hydroxyethyl)amino]-1*H*-benz[*de*]-isoquinoline-1,3(2*H*)-dione (1). A solution of **3a** (0.7 g, 2.52 mmol) and 2-aminoethanol (1.5 mL, 25.26 mmol) in 12.5 mL of NMP was stirred at 200 °C under microwave irradiation for 30 min. Addition of water gave a precipitate that was filtered and washed subsequently with EtOH and Et_2O. The crude was crystallized from acetone to give **1** (0.28 g, 27%) as a yellow solid. ^{1}H NMR (300 MHz, DMSO-d_6) δ 8.77 (d, J = 8.4 Hz, 1H), 8.45 (d, J = 7.2 Hz, 1H), 8.27 (d, J = 8.4 Hz, 1H), 7.84−7.79 (m, 1H), 7.66−7.64 (m, 2H), 7.50−7.46 (m, 1H), 7.37 (d, J = 7.6 Hz, 1H), 7.31 (dd, J = 8.4, 7.2 Hz, 1H), 6.87 (d, J = 8.8 Hz, 1H), 4.92−4.90 (m, 1H), 3.75−3.71 (m, 2H), 3.53−3.49 (m, 2H); ^{13}C NMR (100 MHz, DMSO-d_6) δ 163.8, 162.9, 151.0, 138.2, 134.3, 132.2, 130.8, 130.5, 129.9, 128.8, 128.6, 124.2, 122.1, 121.0, 120.2, 107.7, 103.9, 58.8, 45.9; HRMS (ESI) m/z calcd for $C_{20}H_{16}BrN_2O_3$ 411.0339, found 411.0332; RP-HPLC method 1, t_R = 1.07 min; method 2, t_R = 1.63 min.

6-[(2-Hydroxyethyl)amino]-2-phenyl-1*H*-benzo[*de*]isoquinoline-1,3(2*H*)-dione (4). A solution of 4-bromo-1,8-naphthalic anhydride **2a** (330 mg, 1.20 mmol) in NMP (2 mL) was treated with aniline (0.16 mL, 1.80 mmol). The reaction mixture was stirred at 200 °C under microwave irradiation for 30 min. Addition of water gave a precipitate that was purified by silica gel chromatography (5−10% acetone/toluene gradient), giving 210 mg of 6-bromo-2-phenyl-1*H*-benzo[*de*]isoquinoline-1,3(2*H*)-dione **3b**. A solution of this intermediate (0.6 mmol) in NMP (2 mL) was treated with 2-aminoethanol (0.05 mL, 0.9 mmol) and stirred at 200 °C under microwave irradiation for 30 min. After cooling down, the reaction mixture was purified by RP-HPLC (conditions: Waters X-TERRA MS C_{18}, 5 μm, 19 mm × 150 mm; flow of 20 mL/min; gradient, (A) H_2O + 0.1% TFA, (B) MeCN + 0.1% TFA, 99% A isocratic for 2 min, linear to 1% A in 10 min, 1% A isocratic for 5 min) to give **5** (61 mg, 38%) as a solid. ^{1}H NMR (400 MHz, DMSO-d_6) δ 8.76 (d, J = 8.5 Hz, 1H), 8.44 (d, J = 7.2 Hz, 1H), 8.26 (d, J = 8.5 Hz, 1H), 7.79−7.76 (m, 1H), 7.72 (t, J = 7.9 Hz, 1H), 7.52−7.48 (m, 2H), 7.43 (t, J = 7.2 Hz, 1H), 7.30 (d, J = 7.4 Hz, 2H), 6.85 (d, J = 8.5 Hz, 1H), 4.91 (br s, 1H), 3.74−3.71 (m, 2H), 3.52−3.49 (m, 2H); ^{13}C NMR (75 MHz, DMSO-d_6) δ 163.4, 162.6, 150.4, 136.0, 133.7, 130.2, 129.4, 128.7, 128.1, 127.2, 123.7, 121.7, 119.7, 107.3, 103.3, 58.3, 45.0; HRMS (ESI) m/z calcd for $C_{20}H_{17}N_2O_3$ 333.1233, found 333.1234; RP-HPLC method 1, t_R = 0.77 min; method 2, t_R = 1.32 min.

2-(3-Bromophenyl)-1*H*-benzo[*de*]isoquinoline-1,3(2*H*)-dione (5). In a manner identical to that described above for the preparation of **3a**, 1,8-naphthalic anhydride **2b** (324 mg, 1.63 mmol) was treated with 3-bromoaniline (0.27 mL, 2.45 mmol) to give **5** (383 mg, 67%) as a solid. ^{1}H NMR (400 MHz, DMSO-d_6) δ 8.86 (d, J = 8.3 Hz, 1H), 8.48 (d, J = 8.1 Hz, 1H), 8.23 (d, J = 8.3 Hz, 1H), 8.00 (d, J = 8.3 Hz, 1H), 7.90−7.86 (m, 1H), 7.82−7.78 (m, 2H), 7.67 (d, J = 7.2 Hz, 1H), 7.55−7.53 (m, 2H); ^{13}C NMR (75 MHz, DMSO-d_6) δ 167.8, 167.0, 136.2, 135.7, 133.4, 131.0, 130.7, 130.0, 129.2, 129.0, 127.3, 126.4, 123.9, 121.1, 118.6; HRMS (ESI) m/z calcd for $C_{18}H_{11}BrNO_2$ 351.9970, found 351.9962; RP-HPLC method 1, t_R = 1.86 min; method 2, t_R = 2.35 min.

6-Amino-2-(3-bromophenyl)-1*H*-benzo[*de*]isoquinoline-1,3(2*H*)-dione (6). A solution of 6-amino-1*H*,3*H*-benzo[*de*]isochromene-1,3-dione **2c** (50 mg, 0.23 mmol) and TEA (0.16 mL, 1.16 mmol) in DMF (1 mL) was treated with 3-bromoaniline (0.13 mL, 1.17 mmol). The reaction mixture was stirred at 230 °C under microwave irradiation for 3 h. The resulting precipitate was filtered, washed with Et_2O, and dried to give **6** (18 mg, 21%) as a pale-yellow powder. ^{1}H NMR (400 MHz, DMSO-d_6) δ 8.67 (d, J = 8.4 Hz, 1H), 8.44 (d, J = 6.8 Hz, 1H), 8.20 (d, J = 8.4 Hz, 1H), 7.69 (dd, J = 8.4, 6.8 Hz, 1H), 7.66−7.62 (m, 2H), 7.52−7.45 (m, 3H), 6.88 (d, J = 8.4 Hz, 1H); ^{13}C NMR (100 MHz, DMSO-d_6) δ 163.9, 162.9, 152.9, 138.2, 134.0, 132.2, 131.1, 130.8, 130.5, 130.2, 129.6, 128.6, 123.9, 122.1, 121.0, 119.5, 108.1, 107.6; HRMS (ESI) m/z calcd for $C_{18}H_{12}BrN_2O_2$ 367.0077, found 367.0071; RP-HPLC method 1, t_R = 1.22 min; method 2, t_R = 1.70 min.

General Procedure for the Synthesis of 7−9, 15−17, and 19. A solution of **3a** (80 mg, 0.19 mmol) in NMP (0.9 mL) was treated with the appropriate amine (10 equiv). The reaction mixture was stirred at 200 °C under microwave irradiation for 30 min. Addition of water (2 mL) afforded a precipitate that was isolated by filtration to give **7−9**, **15−17**, and **19**.

2-(3-Bromophenyl)-6-(ethylamino)-1*H*-benzo[*de*]isoquinoline-1,3(2*H*)-dione (9). Yield 57%; ^{1}H NMR (300 MHz, DMSO-d_6) δ 8.76 (d, J = 8.2 Hz, 1H), 8.44 (d, J = 7.1 Hz, 1H), 8.27 (d, J = 8.6 Hz, 1H), 7.83−7.79 (m, 1H), 7.71 (dd, J = 8.2, 7.1 Hz, 1H), 7.46−7.44 (m, 3H), 7.38−7.35 (m, 1H), 7.37 (d, J = 8.0 Hz, 1H), 6.82 (d, J = 8.8 Hz, 1H), 3.46−3.42 (m, 2H), 1.33 (t, J = 7.1 Hz, 3H); ^{13}C NMR (100 MHz, DMSO-d_6) δ 163.8, 162.9, 150.7, 138.2, 134.3, 132.2, 130.8, 130.5, 129.9, 128.8, 128.6, 124.1, 122.1, 121.0, 120.2, 107.6, 103.7, 37.6, 13.6; HRMS (ESI) m/z calcd for $C_{20}H_{16}BrN_2O_2$ 395.0386, found 395.0390; RP-HPLC method 1, t_R = 1.54 min; method 2, t_R = 2.01 min.

2-(3-Bromophenyl)-6-[(2-hydroxyethyl)(methyl)amino]-1*H*-benzo[*de*]isoquinoline-1,3(2*H*)-dione (8). Yield 45%; ^{1}H NMR (400 MHz, DMSO-d_6) δ 8.78 (d, J = 8.6 Hz, 1H), 8.46 (d, J = 6.8 Hz, 1H), 8.35 (d, J = 8.2 Hz, 1H), 7.78 (dd, J = 8.6, 6.8 Hz, 1H), 7.66−7.65 (m, 2H), 7.50−7.40 (m, 2H), 7.33 (d, J = 8.4 Hz, 1H), 4.89−4.87 (m, 1H), 3.79−3.77 (m, 2H), 3.48−3.45 (m, 2H), 3.30 (s, 3H); ^{13}C NMR (100 MHz, DMSO-d_6) δ 163.8, 163.1, 156.9, 137.8, 132.2, 132.1, 131.8, 130.9, 130.6, 130.1, 128.5, 124.9, 124.7, 122.7, 121.1, 114.1, 113.7, 59.3, 58.3; HRMS (ESI) m/z calcd for

$C_{21}H_{18}BrN_2O_3$ 425.0491, found 425.0495; RP-HPLC method 1, t_R = 1.22 min; method 2, t_R = 1.79 min.

2-(3-Bromophenyl)-6-[(2-methoxyethyl)amino]-1*H*-benzo[*de*]-isoquinoline-1,3(2*H*)-dione (9). Yield 36%; ^{1}H NMR (400 MHz, DMSO-d_6 + TFA) δ 8.77 (d, J = 8.4 Hz, 1H), 8.45 (d, J = 7.2 Hz, 1H), 8.27 (d, J = 8.4 Hz, 1H), 7.86 (br s, 1H), 7.73 (dd, J = 8.4, 7.2 Hz, 1H), 7.66−7.64 (m, 2H), 7.50−7.46 (m, 1H), 7.37 (d, J = 8.0 Hz, 1H), 6.89 (d, J = 8.8 Hz, 1H), 3.67−3.61 (m, 4H), 3.32 (s, 3H); ^{13}C NMR (100 MHz, DMSO-d_6) δ 163.9, 163.0, 150.8, 138.2, 134.3, 132.2, 130.8, 130.5, 130.0, 128.9, 128.6, 124.3, 122.2, 121.0, 120.2, 107.9, 104.0, 69.7, 58.1, 42.6; HRMS (ESI) m/z calcd for $C_{21}H_{18}BrN_2O_3$ 425.0495, found 425.0502; RP-HPLC method 1, t_R = 1.37 min; method 2, t_R = 1.91 min.

2-(3-Bromophenyl)-6-[(2-methylpropyl)amino]-1*H*-benzo[*de*]-isoquinoline-1,3(2*H*)-dione (15). Yield 48%; ^{1}H NMR (300 MHz, DMSO-d_6) δ 8.80 (d, J = 8.4 Hz, 1H), 8.44 (d, J = 7.1 Hz, 1H), 8.25 (d, J = 8.4 Hz, 1H), 7.86−7.82 (m, 1H), 7.72 (dd, J = 8.4, 7.1 Hz, 1H), 7.64−7.60 (m, 2H), 7.48−7.45 (m, 1H), 7.38 (d, J = 8.0 Hz, 1H), 6.83 (d, J = 8.6 Hz, 1H), 3.24−3.22 (m, 2H), 2.18−2.02 (m, 1H), 0.99 (d, J = 6.4 Hz, 6H); ^{13}C NMR (100 MHz, DMSO-d_6) δ 163.9, 162.9, 151.0, 138.2, 134.3, 132.1, 130.7, 130.5, 130.0, 128.8, 128.6, 124.2, 122.2, 121.0, 120.2, 107.5, 103.9, 50.4, 26.8, 20.3; HRMS (ESI) m/z calcd for $C_{22}H_{20}BrN_2O_2$ 422.0708, found 422.0724; RP-HPLC method 1, t_R = 1.79 min; method 2, t_R = 2.24 min.

2-(3-Bromophenyl)-6-(cyclohexylamino)-1*H*-benzo[*de*]isoquinoline-1,3(2*H*)-dione (16). Yield 40%; ^{1}H NMR (300 MHz, DMSO-d_6) δ 8.85 (d, J = 8.4 Hz, 1H), 8.43 (d, J = 7.3 Hz, 1H), 8.24 (d, J = 8.6 Hz, 1H), 7.70 (dd, J = 8.4, 7.3 Hz, 1H), 7.54−7.46 (m, 2H), 7.49−7.34 (m, 3H), 6.89 (d, J = 8.8 Hz, 1H), 3.67 (br s, 1H), 2.10−1.99 (m, 2H), 1.82−1.78 (m, 3H), 1.42−1.15 (m, 5H); ^{13}C NMR (100 MHz, DMSO-d_6) δ 163.9, 162.9, 149.9, 138.2, 134.3, 132.2, 130.8, 130.5, 130.1, 129.2, 128.6, 132.9, 122.0, 121.0, 120.2, 107.4, 104.2, 51.5, 31.8, 25.3, 24.7; HRMS (ESI) m/z calcd for $C_{24}H_{22}BrN_2O_2$ 449.0854, found 449.0856; RP-HPLC method 1, t_R = 1.96 min; method 2, t_R = 2.38 min.

2-(3-Bromophenyl)-6-{[2-(methylamino)ethyl]amino}-1*H*-benzo[*de*]isoquinoline-1,3(2*H*)-dione (17). Yield 71%; ^{1}H NMR (400 MHz, DMSO-d_6) δ 8.70 (d, J = 8.4 Hz, 1H), 8.63 (br s, 2H), 8.48 (d, J = 7.2 Hz, 1H), 8.31 (d, J = 8.4 Hz, 1H), 7.82−7.70 (m, 2H), 7.67−7.65 (m, 2H), 7.51−7.47 (m, 1H), 7.38 (d, J = 7.6 Hz, 1H), 6.93 (d, J = 8.4 Hz, 1H), 3.74−3.72 (m, 2H), 3.38−3.29 (m, 2H), 2.68 (s, 3H); ^{13}C NMR (100 MHz, DMSO-d_6) δ 163.8, 163.0, 150.2, 138.0, 134.0, 132.2, 130.9, 130.5, 129.8, 129.0, 128.6, 124.5, 122.2, 121.1, 120.5, 108.9, 104.1, 46.4, 32.6; HRMS (ESI) m/z calcd for $C_{21}H_{19}BrN_3O_2$ 424.0651, found 424.0659; RP-HPLC method 1, t_R = 0.3 min; method 2, t_R = 1.15 min.

1-Benzyl-4-{[2-(3-bromophenyl)-1,3-dioxo-2,3-dihydro-1*H*-benzo[*de*]isoquinolin-6-yl]amino}piperidinium Trifluoroacetate (19). After cooling down, the reaction mixture was purified by RP-HPLC (conditions: Waters X-TERRA MS C_{18}, 5 μm, 19 mm × 150 mm; flow of 20 mL/min; gradient, (A) H_2O + 0.1% TFA, (B) MeCN + 0.1% TFA, 99% A isocratic for 2 min, linear to 1% A in 10 min, 1% A isocratic for 5 min) to give **5** (17 mg, 14%). ^{1}H NMR (300 MHz, DMSO-d_6 + TFA) δ 9.70 (br s, 1H), 8.84 (d, J = 8.2 Hz, 1H), 8.45 (d, J = 7.3 Hz, 1H), 8.25 (d, J = 8.6 Hz, 1H), 7.71 (dd, J = 8.2, 7.3 Hz, 1H), 7.69−7.64 (m, 2H), 7.53−7.43 (m, 7H), 7.35 (d, J = 7.9 Hz, 1H), 6.96 (d, J = 8.8 Hz, 1H), 4.37 (br s, 2H), 3.96−3.80 (m, 1H), 3.58−3.50 (m, 2H), 3.22−3.10 (m, 2H), 2.31−2.22 (m, 2H), 1.98−1.89 (m, 2H); ^{13}C NMR (100 MHz, DMSO-d_6) δ 163.8, 162.9, 149.6, 138.0, 134.0, 132.1, 121.5, 130.9, 130.5, 129.9, 129.6, 129.4, 129.3, 128.8, 128.6, 124.3, 122.2, 121.0, 120.3, 108.4, 104.6, 59.0, 50.6, 47.6, 28.3; HRMS (ESI) m/z calcd for $C_{30}H_{27}BrN_3O_2$ 540.1281, found 540.1296; RP-HPLC method 1, t_R = 0.61 min; method 2, t_R = 1.40 min.

2-(3-Bromophenyl)-7-[(2-hydroxyethyl)amino]-2,3-dihydro-1*H*-benzo[*de*]isoquinolin-1-one (10). A solution of **1** (50 mg, 0.12 mmol) in EtOH/H_2O (10:1) (6 mL) was treated with sodium borohydride (23 mg, 0.61 mmol) at room temperature. The reaction mixture was stirred overnight, quenched with 1 N HCl, and extracted with EtOAc. The combined organic layers were dried and filtered, and the filtrate was concentrated in vacuo to yield the crude product that was purified by RP-HPLC (conditions: Waters X-TERRA MS C_{18}, 5 μm, 19 mm × 150 mm; flow of 20 mL/min; gradient, (A) H_2O + 0.1% TFA, (B) MeCN + 0.1% TFA, 90% A isocratic for 2 min, linear to 30% A in 10 min, then linear to 0% A in 2 min) to give **10** (13 mg, 26%) as a solid. ^{1}H NMR (300 MHz, DMSO-d_6) δ 8.13 (m, 1H), 8.06 (d, J = 8.4 Hz, 1H), 7.74 (s, 1H), 7.53−7.40 (m, 5H), 6.91 (br s, 1H), 6.68 (d, J = 8.4 Hz, 1H), 5.29 (s, 2H), 4.83 (t, J = 5.5 Hz, 1H), 3.73−3.67 (m, 2H), 3.41 (m, 2H); ^{13}C NMR (100 MHz, DMSO-d_6) δ 162.8, 148.0, 144.5, 130.3, 129.2, 128.7, 128.5, 124.9, 124.1, 123.1, 121.1, 120.5, 120.1, 111.4, 102.3, 58.9, 52.5, 45.5; HRMS (ESI) m/z calcd for $C_{20}H_{18}BrN_2O_2$ 397.0546, found 397.0540; RP-HPLC method 1, t_R = 1.16 min; method 2, t_R = 1.73 min.

2-{[2-(3-Bromophenyl)-2,3-dihydro-1*H*-benzo[*de*]isoquinolin-6-yl]amino}ethanol (11). BH_3 (0.93 mL, 1 M solution in THF) was added dropwise to a solution of **1** (50 mg, 0.12 mmol) in THF (1.2 mL) under nitrogen atmosphere. The reaction mixture was stirred to reflux for 5 h. After cooling to 0 °C, the reaction was carefully quenched by dropwise addition of MeOH until hydrogen evolution ceased. The mixture was concentrated in vacuo to give a residue that was diluted with 6 N HCl (0.5 mL) and stirred to reflux for 30 min. After cooling to room temperature, the mixture was basified with 2 N NaOH. The aqueous phase was extracted with EtOAc. The combined organic layers were dried and filtered and the filtrate was concentrated in vacuo to yield the crude product that was purified by silica gel chromatography (10−70% EtOAc/petroleum ether gradient) to give **11** (16 mg, 34%) as a solid. ^{1}H NMR (400 MHz, DMSO-d_6) δ 7.97 (d, J = 7.8 Hz, 1H), 7.37 (m, 2H), 7.23−7.20 (m, 2H), 7.12−7.10 (m, 2H), 6.86−6.84 (m, 1H), 6.49 (d, J = 7.6 Hz, 1H), 5.89−5.86 (m, 1H), 4.78 (s, 2H), 4.69 (s, 2H), 3.70−3.66 (m, 2H), 3.28−3.24 (m, 2H); ^{13}C NMR (100 MHz, DMSO-d_6) δ 151.8, 143.0, 132.1, 130.6, 128.4, 123.7, 123.4, 122.6, 122.4, 120.7, 120.1, 118.7, 118.1, 114.9, 102.5, 59.2, 51.7, 51.3, 45.9; HRMS (ESI) m/z calcd for $C_{20}H_{20}BrN_2O$ 381.0680, found 381.0679; RP-HPLC method 1, t_R = 0.71 min; method 2, t_R = 1.29 min.

General Procedure for the Synthesis of 12−14. A solution of **2a** (100 mg, 0.36 mmol) in EtOH (2 mL) was treated with the appropriate aniline (6 equiv). The reaction mixture was stirred at 150 °C under microwave irradiation for 4 h. The resulting precipitate was filtered, affording a crude that was diluted in NMP (1 mL). After addition of 2-aminoethanol (0.066 mL, 1.08 mmol) the resulting solution was stirred at 200 °C under microwave irradiation for 30 min and purified by RP-HPLC (conditions: Waters X-TERRA MS C_{18}, 5 μm, 19 mm × 150 mm; flow of 20 mL/min; gradient, (A) H_2O + 0.1% TFA; (B) MeCN + 0.1% TFA, 99% A isocratic for 2 min, linear to 1% A in 10 min, 1% A isocratic for 5 min) to give **12−14**.

2-(3-Chlorophenyl)-6-[(2-hydroxyethyl)amino]-1*H*-benzo[*de*]-isoquinoline-1,3(2*H*)-dione (12). Yield, 20%; ^{1}H NMR (400 MHz, DMSO-d_6) δ 8.75 (d, J = 7.9 Hz, 1H), 8.44 (d, J = 7.2 Hz, 1H), 8.26 (d, J = 8.6 Hz, 1H), 7.80−7.76 (m, 1H), 7.74−7.70 (m, 1H), 7.54−7.50 (m, 3H), 7.34−7.31 (m, 1H), 6.85 (d, J = 8.6 Hz, 1H), 3.74−3.71 (m, 2H), 3.52−3.48 (m, 2H); ^{13}C NMR (75 MHz, DMSO-d_6) δ 163.8, 162.9, 151.0, 138.0, 134.3, 132.8, 130.8, 130.2, 130.0, 129.4, 128.9, 128.2, 127.9, 124.2, 122.2, 120.2, 107.7, 103.9, 58.8, 45.6; HRMS (ESI) m/z calcd for $C_{20}H_{16}ClN_2O_3$ 367.0844, found 367.0836; RP-HPLC method 1, t_R = 1.02 min; method 2, t_R = 1.58 min.

2-(3-Fluorophenyl)-6-[(2-hydroxyethyl)amino]-1*H*-benzo[*de*]-isoquinoline-1,3(2*H*)-dione (13). Yield, 61%; ^{1}H NMR (400 MHz, DMSO-d_6) δ 8.75 (d, J = 8.6 Hz, 1H), 8.44 (d, J = 7.4 Hz, 1H), 8.26 (d, J = 8.5 Hz, 1H), 7.80−7.76 (m, 1H), 7.74−7.70 (m, 1H), 7.54−7.50 (m, 1H), 7.30−7.28 (m, 2H), 7.19 (d, J = 7.9 Hz, 1H), 6.85 (d, J = 8.5 Hz, 1H), 3.74−3.71 (m, 2H), 3.52−3.48 (m, 2H); ^{13}C NMR (75 MHz, DMSO-d_6) δ 163.8, 162.9, 151.0, 138.2 (d, J = 10.5 Hz), 134.2, 130.8, 130.1, 130.0, 129.9, 128.8, 125.6, 124.2, 122.1, 120.2, 116.7 (d, J = 22.5 Hz), 114.7 (d, J = 20.0 Hz), 107.7,

103.9, 58.8, 45.6; HRMS (ESI) m/z calcd for $C_{20}H_{16}FN_2O_3$ 351.1139, found 351.1133; RP-HPLC method 1, t_R = 0.86 min; method 2, t_R = 1.42 min.

3-{6-[(2-Hydroxyethyl)amino]-1,3-dioxo-1*H*-benzo[*de*]isoquinolin-2(3*H*)-yl}benzenesulfonamide (14). Yield, 75%; ^{1}H NMR (400 MHz, DMSO-d_6) δ 8.77 (d, J = 8.6 Hz, 1H), 8.45 (d, J = 7.2 Hz, 1H), 8.27 (d, J = 8.6 Hz, 1H), 7.89 (d, J = 7.9 Hz, 1H), 7.82 (br s, 1H), 7.78 (br s, 1H), 7.75−7.69 (m, 2H), 7.58 (d, J = 7.9 Hz, 1H), 7.48 (br s, 2H), 6.87 (d, J = 8.5 Hz, 1H), 3.74−3.71 (m, 2H), 3.52−3.48 (m, 2H); ^{13}C NMR (75 MHz, DMSO-d_6) δ 164.0, 163.0, 151.1, 144.8, 136.9, 134.3, 132.9, 130.8, 130.0, 129.4, 128.9, 126.5, 125.2, 124.2, 122.1, 120.3, 107.6, 103.9, 58.8, 45.6; HRMS (ESI) m/z calcd for $C_{20}H_{18}BrN_3O_5S$ 412.0962, found 412.0957; RP-HPLC method 1, t_R = 0.54 min; method 2, t_R = 1.04 min.

4-{[2-(3-Bromophenyl)-1,3-dioxo-2,3-dihydro-1*H*-benzo[*de*]-isoquinolin-6-yl]amino}piperidinium Trifluoroacetate (18). A solution of **3a** (70 mg, 0.162 mmol) in NMP (0.8 mL) was treated with *tert*-butyl 4-aminopiperidine-1-carboxylate (228 mg, 1.14 mmol). The reaction mixture was stirred at 250 °C under microwave irradiation for 20 min. Addition of water (2 mL) gave a precipitate that was filtered, affording a crude that was diluted in 0.5 mL of CH_2Cl_2/TFA (2:1) (0.5 mL), and the resulting solution was stirred at room temperature for 15 min and concentrated in vacuo to obtain a residue that was purified by RP-HPLC (conditions: Waters X-TERRA MS C_{18}, 5 μm, 19 mm × 150 mm; flow of 20 mL/min; gradient, (A) H_2O + 0.1% TFA, (B) MeCN + 0.1% TFA, 90% A isocratic for 2 min, linear to 30% A in 10 min, then linear to 0% A in 2 min) to give **18** (16 mg, 39%) as a solid. ^{1}H NMR (500 MHz, DMSO-d_6) δ 8.87 (d, J = 8.5 Hz,1H), 8.60 (br s, 1H), 8.47 (d, J = 7.0 Hz, 1H), 8.42 (br s, 1H), 8.28 (d, J = 8.5 Hz, 1H), 7.77 (dd, J = 8.4, 7.0 Hz, 1H), 7.67−7.64 (m, 2H), 7.57−7.55 (m, 1H), 7.50−7.47 (m, 1H), 6.99 (d, J = 8.8 Hz, 1H), 4.08−3.98 (m, 1H), 3.45−3.42 (m, 2H), 3.14−3.08 (m, 2H), 2.20−2.18 (m, 2H), 1.88−1.82 (m, 2H); ^{13}C NMR (100 MHz, DMSO-d_6) δ 163.8, 162.9, 149.5, 138.0, 134.0, 132.2, 130.8, 130.5, 130.0, 129.3, 128.6, 124.3, 121.0, 120.4, 108.4, 104.5, 47.3, 42.5, 27.9; HRMS (ESI) m/z calcd for $C_{23}H_{21}BrN_3O_2$ 450.0811, found 450.0812; RP-HPLC method 1, t_R = 0.30 min; method 2, t_R = 1.22 min.

***cis*-4-{[2-(3-Bromophenyl)-1,3-dioxo-2,3-dihydro-1*H*-benzo[*de*]-isoquinolin-6-yl]amino}cyclohexanecarboxylic Acid (20).** In a manner identical to that described above for the preparation of **1**, reaction of **3a** (43 mg, 0.1 mmol) and *cis*-4-aminocyclohexanecarboxylic acid (43 mg, 0.3 mmol) gave **20** (5 mg, 10%). ^{1}H NMR (400 MHz, DMSO-d_6) δ 12.22 (br s, 1H), 8.86 (d, J = 8.5 Hz, 1H), 8.43 (d, J = 7.2 Hz, 1H), 8.24 (d, J = 8.7 Hz, 1H), 7.74−7.59 (m, 3H), 7.50−7.34 (m, 3H), 6.90 (d, J = 8.7 Hz, 1H), 3.81−3.70 (m, 1H), 2.63−2.56 (m, 1H), 2.16−2.03 (m, 2H), 1.94−1.82 (m, 2H), 1.76−1.62 (m, 3H); ^{13}C NMR (100 MHz, DMSO-d_6) δ 175.9, 163.9, 162.9, 150.0, 138.2, 134.3, 132.2, 130.8, 130.5, 130.1, 129.3, 128.6, 124.1, 122.1, 121.0, 120.3, 107.6, 104.3, 50.3, 38.3, 28.3, 25.4; HRMS (ESI) m/z calcd for $C_{25}H_{22}BrN_2O_4$ 493.0757, found 493.0765; RP-HPLC method 1, t_R = 1.44 min; method 2, t_R = 1.93 min.

Acknowledgment. We thank Maria-Cecilia Palumbi for automated RP-HPLC purification, Cinzia Volpari for crystallization experiments, Dr. Odalys Gonzalez Paz for pharmacokinetic studies, Monica Bisbocci for biological testing, Dr. Silvia Pesci for NMR spectrometry, Dr. Charles W. Ross and Claudio Giuliano for HRMS determinations, and Dr. Jorg Habermann for preparation of **21**.

Supporting Information Available: Enzyme and cell-based assay protocols, pharmacokinetic studies, soaking experiments, and X-ray data collection, structure determination, and refinement description. This material is available free of charge via the Internet at http://pubs.acs.org.

References

(1) WHO, January **2006**, posting date.
(2) Field, J. J.; Hoofnagle, J. H. Mechanism of Action of Interferon and Ribavirin in Treatment of Hepatitis C. *Nature* **2005**, *436*, 967–972.
(3) (a) Soriano, V.; Madejon, A.; Vispo, E.; Labarga, P.; Garcia-Samaniego, J.; Martin-Carbonero, L.; Sheldon, J.; Bottecchia, M.; Tuma, P.; Barreiro, P. Emerging Drugs for Hepatitis C. *Expert Opin. Emerging Drugs* **2008**, *13*, 1–19. (b) Kwong, A. D.; Mc Nair, L.; Jacobsen, I.; George, S. Recent Progress in the Development of Selected Hepatitis C Virus NS3-4A Protease and NS5B Polymerase Inhibitors. *Curr. Opin. Pharmacol.* **2008**, *8*, 522–531. (c) Beaulieu, P. L. Recent Advances in the Development of NS5B Polymerase Inhibitors for the Treatment of Hepatitis C Virus Infection. *Expert Opin. Ther. Pat.* **2009**, *19*, 145–164.
(4) Reed, K. E.; Rice, C. M. Overview of Hepatitis C Virus Genome Structure, Polyprotein Processing, and Protein Properties. *Curr. Top. Microbiol. Immunol.* **2000**, *242*, 55–84.
(5) (a) Ago, H.; Adachi, T.; Yoshida, A.; Yamamoto, M.; Habuka, N.; Yatsunami, K.; Miyano, M. Crystal Structure of the RNA-Dependent RNA Polymerase of Hepatitis C Virus. *Structure* **1999**, *7*, 1417–1426. (b) Bressanelli, S.; Tomei, L.; Roussel, A.; Incitti, I.; Vitale, R. L.; Mathieu, M.; De Francesco, R.; Rey, F. A. Crystal Structure of the RNA-Dependent RNA Polymerase of Hepatitis C Virus. *Proc. Natl. Acad. Sci. U.S.A.* **1999**, *96*, 13034–13039. (c) Lesburg, C. A.; Cable, M. B.; Ferrari, E.; Hong, Z.; Mannarino, A. F.; Weber, P. C. Crystal Structure of the RNA-Dependent RNA Polymerase from Hepatitis C Virus Reveals a Fully Encircled Active Site. *Nat. Struct. Biol.* **1999**, *6*, 937–943. (d) Bressanelli, S.; Tomei, L.; Rey, F. A.; De Francesco, R. Structural Analysis of the Hepatitis C Virus RNA Polymerase in Complex with Ribonucleotides. *J. Virol.* **2002**, *76*, 3482–3492. (e) O'Farrell, D.; Trowbridge, R.; Rowlands, D.; Jager, J. Substrate Complexes of Hepatitis C Virus RNA Polymerase (HC-J4): Structural Evidence for Nucleotide Import and De-Novo Initiation. *J. Mol. Biol.* **2003**, *326*, 1025–1035. (f) Biswal, B. K.; Cherney, M. M.; Wang, M.; Chan, L.; Yannopoulos, C. G.; Bilimoria, D.; Nicolas, O.; Bedard, J.; James, M. N. Crystal Structures of the RNA-Dependent RNA Polymerase Genotype 2a of Hepatitis C Virus Reveal Two Conformations and Suggest Mechanisms of Inhibition by Non-Nucleoside Inhibitors. *J. Biol. Chem.* **2005**, *280*, 18202–18210. (g) Rydberg, E. H.; Cellucci, A.; Bartholomew, L.; Mattu, M.; Barbato, G.; Ludmerer, S. W.; Graham, D. J.; Altamura, S.; Paonessa, G.; De Francesco, R.; Migliaccio, G.; Carfi, A. Structural Basis for Resistance of the Genotype 2b Hepatitis C Virus NS5B Polymerase to Site A Non-Nucleoside Inhibitors. *J. Mol. Biol.* **2009**, *390*, 1048–1059.
(6) (a) Koch, U.; Narjes, F. Recent Progress in the Development of Inhibitors of the Hepatitis C Virus RNA-Dependent RNA Polymerase. *Curr. Top. Med. Chem.* **2007**, *7*, 1302–1329. (b) De Francesco, R.; Carfi, A. Advances in the Development of New Therapeutic Agents Targeting the NS3-4A Serine Protease or the NS5B RNA-Dependent RNA Polymerase of the Hepatitis C Virus. *Adv. Drug. Delivery Rev.* **2007**, *59*, 1242–1262.
(7) (a) Tomei, L.; Altamura, S.; Bartholomew, L.; Biroccio, A.; Ceccacci, A.; Pacini, L.; Narjes, F.; Gennari, N.; Bisbocci, M.; Incitti, I.; Orsatti, L.; Harper, S.; Stansfield, I.; Rowley, M.; De Francesco, R.; Migliaccio, G. Mechanism of Action and Antiviral Activity of Benzimidazole-Based Allosteric Inhibitors of the Hepatitis C Virus RNA-Dependent RNA Polymerase. *J. Virol.* **2003**, *77*, 13225–13231. (b) Di Marco, S.; Volpari, C.; Tomei, L.; Altamura, S.; Harper, S.; Narjes, F.; Koch, U.; Rowley, M.; De Francesco, R.; Migliaccio, G.; Carfi, A. Interdomain Communication in Hepatitis C Virus Polymerase Abolished by Small Molecule Inhibitors Bound to a Novel Allosteric Site. *J. Biol. Chem.* **2005**, *280*, 29765–29770. (c) Harper, S.; Pacini, B.; Avolio, S.; Di Filippo, M.; Migliaccio, G.; Laufer, R.; De Francesco, R.; Rowley, M.; Narjes, F. Development and Preliminary Optimization of Indole-N-acetamide Inhibitors of Hepatitis C Virus NS5B Polymerase. *J. Med. Chem.* **2005**, *48*, 1314–1317. (d) Kukolj, G.; McGibbon, G. A.; McKercher, G.; Marquis, M.; Lefebvre, S.; Thauvette, L.; Gauthier, J.; Goulet, S.; Poupart, M. A.; Beaulieu, P. L. Binding Site Characterization and Resistance to a Class of Non-Nucleoside Inhibitors of the Hepatitis C Virus NS5B Polymerase. *J. Biol. Chem.* **2005**, *280*, 39260–39267. (e) Liu, Y.; Donner, P. L.; Pratt, J. K.; Jiang, W. W.; Ng, T.; Gracias, V.; Baumeister, S.; Wiedeman, P. E.; Traphagen, L.; Warrior, U.; Maring, C.; Kati, W. M.; Djuric, S. W.; Molla, A. Identification of Halosalicylamide Derivatives as a Novel Class of Allosteric Inhibitors of HCV NS5B Polymerase. *Bioorg. Med. Chem. Lett.* **2008**, *18*, 3173–3177.
(8) (a) Wang, M.; Ng, K. K.; Cherney, M. M.; Chan, L.; Yannopoulos, C. G.; Bedard, J.; Morin, N.; Nguyen-Ba, N.; Alaoui-Ismaili, M. H.; Bethell, R. C.; James, M. N. Non-Nucleoside Analogue Inhibitors Bind to an Allosteric Site on HCV NS5B Polymerase. *J. Biol. Chem.* **2003**, *278*, 9489–9495. (b) Biswal, B. K.; Wang, M.;

Cherney, M. M.; Chan, L.; Yannopoulos, C. G.; Bilimoria, D.; Bedard, J.; James, M. N. Non-Nucleoside Inhibitors Binding to Hepatitis C Virus NS5B Polymerase Reveal a Novel Mechanism of Inhibition. *J. Mol. Biol.* **2006**, *361*, 33–45. (c) LaPorte, M. G.; Jackson, R. W.; Draper, T. L.; Gaboury, J. A.; Galie, K.; Herbertz, T.; Hussey, A. R.; Rippin, S. R.; Benetatos, C. A.; Chunduru, S. K.; Christensen, J. S.; Coburn, G. A.; Rizzo, C. J.; Rhodes, G.; O'Connell, J.; Howe, A. Y. M.; Mansour, T. S.; Collet, M. S.; Pevear, D. C.; Young, D. C.; Gao, T.; Tyrrell, D. L. J.; Kneteman, N. M.; Burns, C. J.; Condon, S. M. The Discovery of Pyrano[3,4-b]indole-Based Allosteric Inhibitors of HCV NS5B Polymerase with in Vivo Activity. *ChemMedChem* **2008**, *3*, 1508–1515. (d) Li, H.; Tatlock, J.; Linton, A.; Gonzalez, J.; Jewell, T.; Patel, L.; Ludlum, S.; Drowns, M.; Rahavendran, S. V.; Skor, H.; Hunter, R.; Shi, S. T.; Herlihy, K. J.; Parge, H.; Hickey, M.; Yu, X.; Nonomiya, J.; Lewis, C. Discovery of (R)-6-Cyclopentyl-6-(2-(2,6-diethylpyridin-4-yl)ethyl)-3-((5,7-dimethyl-[1,2,4]triazolo[1,5-a]pyrimidin-2-yl)methyl)-4-hydroxy-5,6-dihydropyran-2-one (PF-00868554) as a Potent and Orally Available Hepatitis C Virus Polymerase Inhibitor. *J. Med. Chem.* **2009**, *52*, 1255–1258.

(9) (a) Pfefferkorn, J. A.; Greene, M. L.; Nugent, R. A.; Gross, R. J.; Mitchell, M. A.; Finzel, B. C.; Harris, M. S.; Wells, P. A.; Shelly, J. A.; Anstadt, R. A.; Kilkuskie, R. E.; Kopta, L. A.; Schwende, F. J. Inhibitors of HCV NS5B Polymerase. Part 1: Evaluation of the Southern Region of (2*Z*)-2-(Benzoylamino)-3-(5-phenyl-2-furyl)acrylic Acid. *Bioorg. Med. Chem. Lett.* **2005**, *15*, 2481–2486. (b) Tedesco, R.; Shaw, A. N.; Bambal, R.; Chai, D.; Concha, N. O.; Darcy, M. G.; Dhanak, D.; Fitch, D. M.; Gates, A.; Gerhardt, W. G.; Halegoua, D. L.; Han, C.; Hofmann, G. A.; Johnston, V. K.; Kaura, A. C.; Liu, N.; Keenan, R. M.; Lin-Goerke, J.; Sarisky, R. T.; Wiggall, K. J.; Zimmerman, M. N.; Duffy, K. J. 3-(1,1-Dioxo-2H-(1,2,4)-benzothiadiazin-3-yl)-4-hydroxy-2(1H)-quinolinones, Potent Inhibitors of Hepatitis C Virus RNA-Dependent RNA Polymerase. *J. Med. Chem.* **2006**, *49*, 971–983.

(10) (a) Howe, A. Y. M.; Cheng, H.; Johann, S.; Mullen, S.; Chunduru, S. K.; Young, D. C.; Bard, J.; Chopra, R.; Krishnamurthy, G.; Mansour, T.; O'Connell, J. Molecular Mechanism of Hepatitis C Virus Replicon Variants with Reduced Susceptibility to a Benzofuran Inhibitor, HCV-796. *Antimicrob. Agents Chemother.* **2008**, *52*, 3327–3338. (b) Hang, J. Q.; Yang, Y.; Harris, S. F.; Leveque, V.; Whittington, H. J.; Rajyaguru, S.; Ao-Ieong, G.; McCown, M. F.; Wong, A.; Giannetti, A. M.; Le Pogam, S.; Talamás, F.; Cammack, N.; Nájera, I.; Klumpp, K. Slow Binding Inhibition and Mechanism of Resistance of Non-Nucleoside Polymerase Inhibitors of Hepatitis C Virus. *J. Biol. Chem.* **2009**, *284*, 15517–15529.

(11) Le Pogam, S.; Kang, H.; Harris, S. F.; Leveque, V.; Giannetti, A. M.; Ali, S.; Jiang, W. R.; Rajyaguru, S.; Tavares, G.; Oshiro, C.; Hendricks, T.; Klumpp, K.; Symons, J.; Browner, M. F.; Cammack, N.; Najera, I. Selection and Characterization of Replicon Variants Dually Resistant to Thumb- and Palm-Binding Nonnucleoside Polymerase Inhibitors of the Hepatitis C Virus. *J. Virol.* **2006**, *80*, 6146–6154.

(12) Trozzi, C.; Bartholomew, L.; Ceccacci, A.; Biasiol, G.; Pacini, L.; Altamura, S.; Narjes, F.; Muraglia, E.; Paonessa, G.; Koch, U.; De Francesco, R.; Steinkuhler, C.; Migliaccio, G. In Vitro Selection and Characterization of Hepatitis C Virus Serine Protease Variants Resistant to an Active-Site Peptide Inhibitor. *J. Virol.* **2003**, *77*, 3669–3679.

(13) (a) Ghorbanian, S.; Tyman, J. H. P.; Tychopoulos, V. The Synthesis of Symmetrical and Unsymmetrical Alkylaminonaphthalic-1,8-*N*-alkylimides. *J. Chem. Technol. Biotechnol.* **2000**, *75*, 1127–1134. (b) Alexiou, M. S.; Tyman, J. H. P. The Synthesis of Alkylamino-N-alkylnaphthalic-1,8-imides from 2- and 4-Nitronaphthalic Anhydrides by Nitro Group Displacement. *J. Chem. Res.* **2000**, 208–210.

(14) (a) Xuhong, Q.; Zhenghua, Z.; Kongchang, C. H. The Synthesis, Application and Prediction of Stokes Shift in Fluorescent Dyes Derived from 1,8-Naphthalic Anhydride. *Dyes Pigm.* **1989**, *11*, 13–20. (b) Philipova, T. Synthesis and application of fluorescent dyes on basis of 1,8-naphthalic anhydride. *Rev. Roum. Chim.* **1996**, *41*, 591–600.

(15) Sato, R.; Oikawa, K.; Goto, T.; Saito, M. New and Convenient Synthesis of 2-Substituted 2,3-Dihydro-1*H*-benz[*de*]isoquinolin-1-ones. *Bull. Chem. Soc. Jpn.* **1988**, *61*, 2238–2240.

(16) Tomei, L.; Altamura, S.; Bartholomew, L.; Bisbocci, M.; Bailey, C.; Bosserman, M.; Cellucci, A.; Forte, E.; Incitti, I.; Orsatti, L.; Koch, U.; De Francesco, R.; Olsen, D. B.; Carroll, S. S.; Migliaccio, G. Characterization of the Inhibition of Hepatitis C Virus RNA Replication by Nonnucleosides. *J. Virol.* **2004**, *78*, 938–946.

(17) Halgren, T. A. Potential Energy Functions. *Curr. Opin. Struct. Biol.* **1995**, *5*, 205–210.

(18) *MacroModel*, version 7.0: Schrodinger Inc.; Portland, OR; http://www.schrodinger.com/Products/macromodel.html.

(19) (a) Li, F.; Cui, J.; Guo, L.; Qian, X.; Ren, W.; Wang, K.; Liu, F. Molecular Design, Chemical Synthesis, and Biological Evaluation of "4−1" Pentacyclic Aryl/Heteroaryl-imidazonaphthalimides. *Bioorg. Med. Chem.* **2007**, *15*, 5114–5121. (b) Braña, M. F.; Ramos, A. Naphthalimides as Anti-Cancer Agents: Synthesis and Biological Activity. *Curr. Med. Chem.: Anti-Cancer Agents* **2001**, *1*, 237–255.